

# Band-gap shift in CdS semiconductor by photoacoustic spectroscopy: Evidence of a cubic to hexagonal lattice transition

O. Zelaya-Angel, J. J. Alvarado-Gil, and R. Lozada-Morales

Departamento de Física, Centro de Investigación y Estudios Avanzados, I.P. N., Ap. Postal 14-740, México D. F. 07000, México

H. Vargas

Instituto de Física, Universidade Estadual de Campinas, Caixa Postal 6165, 13081-970 Campinas, S.P., Brazil

A. Ferreira da Silva

Instituto Nacional de Pesquisas Espaciais INPE, Laboratório Associado de Sensores e Materiais/LAS, Caixa Postal 515, 12225 São José dos Campos, Brazil

(Received 21 September 1993; accepted for publication 12 November 1993)

The band-gap energies of the CdS semiconductor are obtained by a photoacoustic spectroscopy (PAS) technique over a range of temperature of thermal annealing (TTA), in which the evolution of the sample structure is characterized by x-ray diffraction patterns. The PAS experiment gives a set of data for the band-gap shift in the region of the fundamental absorption edge. With increasing TTA the band-gap shift increases up to a critical TTA when its slope decreases in a roughly symmetrical way. It is suggested that at this temperature a cubic to hexagonal-lattice transition occurs.

The use of photoacoustic spectroscopy (PAS) has become well established in the past few years mainly due to its importance as a guide in the study of optical properties of semiconductors.<sup>1-4</sup> PAS can lead, for instance, to the value of the band-gap energy, which is an important parameter in electronic and optoelectronic design.<sup>5-11</sup> It is worth saying that less attention has been paid to applications of this technique to investigate the band-gap shift (BGS) of intrinsic and extrinsic semiconductors. In particular, the CdS semiconductor, which presents a highly stable hexagonal structure  $\alpha$ -CdS,<sup>12</sup> can also be obtained in the metastable cubic phase  $\beta$ -CdS.<sup>12-15</sup> Cardona *et al.* by means of reflectivity measurements at room temperature found the optical band gap of the two phases of CdS thin films, and they could not infer any other conclusions except that the energy difference between the cubic and hexagonal CdS energy gap differs less than 0.1 eV.<sup>13</sup> Later on, Balkanski *et al.*<sup>16</sup> found the narrowing of  $E_g$  as a function of temperature, but for Si. Cubic cadmium sulfide films deposited by chemical bath deposition (CBD) have been reported previously by Nagao *et al.*<sup>17</sup> and hexagonal ones by other workers.<sup>18,19</sup> However, for CdS the growth procedures to obtain one phase or the other as well as the BGS along the evolution from the one phase to another are not well known up to now.

In this letter, we investigate by PAS the BGS of CdS cubic phase thin films deposited by CBD, as they go through the as-grown phase to the hexagonal one after thermal annealing. An account of problems involved in obtaining CdS thin films is also reported. Here we shall concentrate on those details which are of relevance to characterize from x-ray diffraction the cubic and hexagonal structure presented.

Cadmium sulfide polycrystalline films of about 0.5  $\mu\text{m}$  thickness were grown on glass substrata (0.7 $\times$ 5 $\times$ 15 mm<sup>3</sup>) by the CBD method, employing the technique proposed by Call,<sup>18</sup> but using CdCl<sub>2</sub> instead of Cd(NO<sub>3</sub>)<sub>2</sub> as an inorganic chemical agent, maintaining the growth solution at 80 °C. The x-ray diffraction scans showed all as-grown films to be

of the cubic CdS structure.<sup>20</sup> The relative intensity of the peaks indicates a preferred orientation along the (111) direction. Thermal annealing of the films was done in Ar gas + S<sub>2</sub> vapor flux at normal pressure. The temperature of the thermal annealing (TTA) were fixed at 240, 300, 360, 470, and 505 °C each for an average time of 50 h.

We present in Fig. 1 the x-ray diffraction patterns of the as-grown and annealed films. The evolution of the sample structure from the as-grown cubic phase to the hexagonal one<sup>20,21</sup> for the sample annealed at 505 °C can be observed. Patterns corresponding to the hexagonal phase show a preferred orientation along the (002) direction. This could be expected because the cubic (111) and the hexagonal (002) lines coincide within 1%. In the inset of Fig. 1, we can appreciate in more detail the x-ray spectra in the 30°–46°

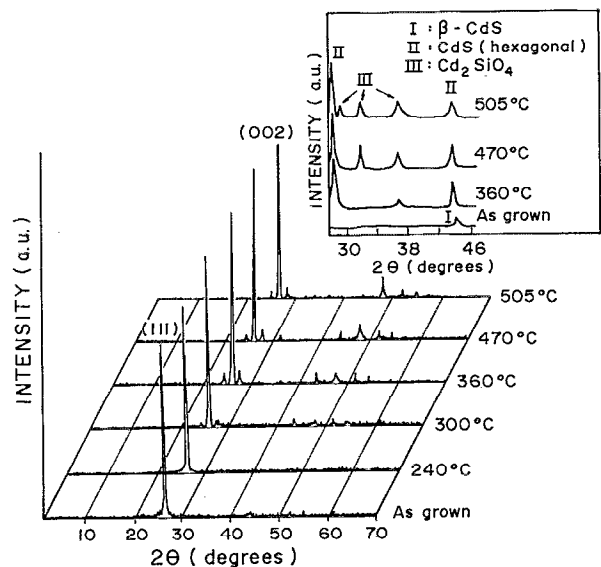


FIG. 1. X-ray diffraction patterns of the as grown and annealed films.

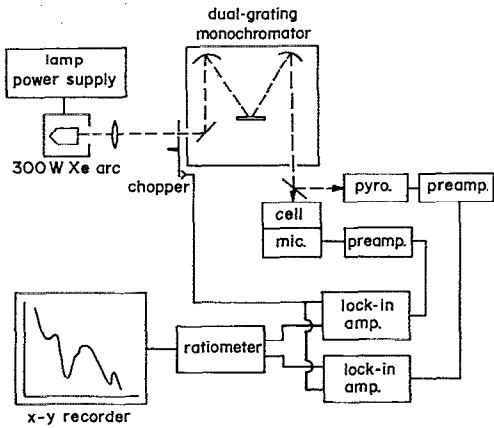


FIG. 2. Block diagram of the photoacoustic spectrometer.

range, where peaks corresponding to  $\text{Cd}_2\text{SiO}_4$  at the interface are present, even though the as-grown sample does not show any such peaks, increasing the x-ray sensitivity these appear. Thermal annealing increases the grain size, so that they become visible, as shown in the inset of Fig. 1. We believe this interface could influence the growth of the cubic structure in this case.

The photoacoustic spectra of the films were obtained in the visible region (300–750 nm) using a commercial EDT model OAS-400 photoacoustic spectrometer. Figure 2 illustrates the operation mode; radiation from an air-cooled high pressure 300 W Xenon arc source, fitted with an integral parabolic reflection optics is focused onto a variable-speed rotating light chopper mounted at the entrance slit of a high-radiance monochromator. The monochromator has two gratings to enable the photoacoustic spectra in the UV-VIS and near-IR regions. A reflective beam splitter passes a fraction of the dispersed radiation to a pyroelectric detector to provide source compensation and a reference signal. Source radiation is then focused onto the photoacoustic cell and sample holder assembly. The photoacoustic signal from the sample cell provides the input to the signal channel lock-in

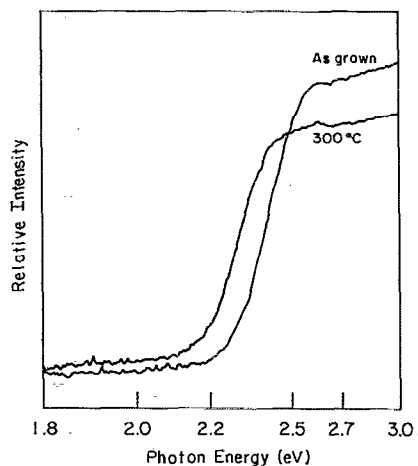


FIG. 3. PA spectra for the as grown and the annealed at 300 °C samples as a function of photon energy.

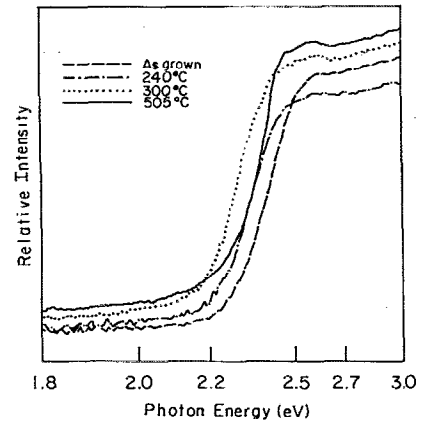


FIG. 4. The PA spectra for different temperature of thermal annealing as a function of photon energy for CdS. The band gap was calculated at the position of the maximum derivative.

amplifier. In a similar manner the output of the pyroelectric is taken to the reference channel lock-in amplifier. The photoacoustic spectra are displayed as a chart recorder for wavelength-dependent signal intensity as shown in Figs. 3 and 4. In this study, the experimental conditions were: chopper modulation frequency, 10 Hz; bandpass 60 nm; time constant, 1 s; scan rate 50 nm/min.

In Fig. 3 we show two typical PAS spectra, one for the as-grown sample and the other for that annealed at 300 °C. The fundamental absorption edge corresponds closely with that previously reported.<sup>2</sup> Each curve exhibits well-expressed changes of the slopes at some points from which the energies are determined. We consider that the band-gap energy is given by the changing of the derivative in the edge. A shift between the two spectra is clearly seen. In Fig. 4 we show the spectra for the whole set of annealed samples. The values of the band gaps for each TTA are shown in Table I.

In Fig. 5 we show the energy gap  $E_g$  as a function of thermal annealing temperature. The energy gap  $E_g$  decreases with increasing TTA, reaching a minimum of 2.28 eV at 300 °C, and then increases rapidly in a roughly symmetrical way with increasing TTA. It is a narrowing-widening-like behavior. Such behavior shows that at this TTA a transition occurs from cubic to hexagonal structure. Newman *et al.*<sup>7</sup> have made measurements of optical absorption in the metastable  $(\text{GaAs})_{1-x}(\text{Ge})_x$  alloy, and observed a similar behavior of  $E_g$  as a function of the composition  $x$ . They found a V-shaped form with a minimum for  $E_g$  at  $x \approx 0.3$  eV, and

TABLE I. Values of the band-gap energy as a function of thermal annealing temperature.

Temperature (°C)	$E_g$ (eV)
80	2.40 ± 0.01
240	2.35 ± 0.01
300	2.28 ± 0.01
360	2.34 ± 0.01
470	2.37 ± 0.01
505	2.38 ± 0.01

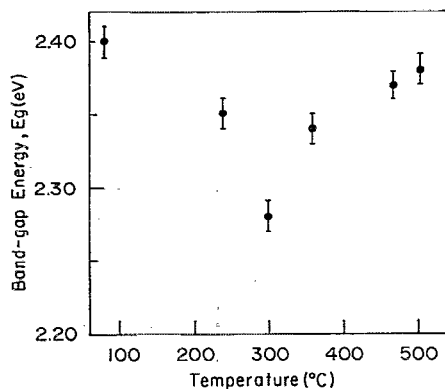


FIG. 5. Band-gap energy dependence on thermal annealing temperature for CdS.

described it as a zinc blende to diamond-lattice order-disorder transition.

In order to investigate the shift of the band gap,  $\Delta E_g$ , as a function of TTA, we define

$$\Delta E_g = E_g(T_0) - E_g(T),$$

where  $T_0 = 80^\circ\text{C}$  is the temperature in the CBD growth process. Here we found  $E_g(T_0) = 2.40\text{ eV}$ . In Fig. 6 we can see the variation in the shift as a function of TTA, the higher shift corresponding to  $\Delta E_g = 120\text{ meV}$  at  $300^\circ\text{C}$ , where the phase transition occurs. The variation of  $\Delta E_g$  in meV is similar to other processes, when concerning its increasing part.<sup>8,10,16</sup>

Many discussions and calculations have attributed part of the shift of the band gap due to thermal expansion and electron-phonon interaction.<sup>22</sup> One should point out, however, that a unified model with a detailed calculation would currently be of much interest.

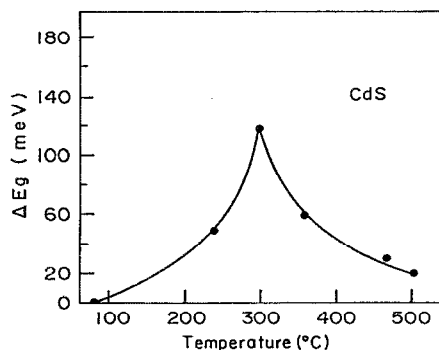


FIG. 6. Band-gap shift  $\Delta E_g$  of CdS as a function of temperature. The full circles correspond to our measurements. The solid line is plotted for a visual effect.

For doped semiconductors the observed band-gap narrowing is associated with different many body effects on the conduction and valence bands.<sup>5-11</sup> Band-gap widening can be understood quantitatively from an effective-mass model.<sup>9</sup> The amount of published work on band-gap shifts in semiconductors is large. One can, for instance, note that oxide semiconductors often possess a large band-gap widening,<sup>9,23</sup> while semiconductors such as Si, Ge, and GaAs may show a band-gap narrowing. There is no study about the above cited behaviors in TTA dependence of the CdS semiconductor.

Investigation of BGS as a function of doping or TTA is very important to optical coating (coating which combines transparency, conductivity, and reflectivity has great importance in basic research and development), transistor design as well as efficiency of solar cells.<sup>5,9,23</sup>

A better understanding of the compensated and uncompensated<sup>24</sup> doping, and temperature dependence are in current progress and will be reported in the future.

In summary, we have shown, by x-ray spectra and band-gap shift, using the PAS technique, that the CdS semiconductor has a critical temperature around  $300^\circ\text{C}$  at which a cubic to hexagonal-lattice transition occurs.

We gratefully acknowledge the Brazilian agencies CNPq and CAPES for financial support. O. Z.-A. and J. J. A.-G. acknowledge a fellowship from CNPq.

- <sup>1</sup> L. Eaves, H. Vargas, and P. J. Williams, *Appl. Phys. Lett.* **38**, 768 (1981).
- <sup>2</sup> A. Mandelis, *Photoacoustic and Thermal Wave Phenomena in Semiconductors* (North-Holland, New York, 1987).
- <sup>3</sup> H. Vargas and L. C. M. Miranda, *Phys. Rep.* **161**, 43 (1988).
- <sup>4</sup> A. Pinto Neto, H. Vargas, N. F. Leite, and L. C. M. Miranda, *Phys. Rev. B* **41**, 9971 (1990).
- <sup>5</sup> K. F. Berggren and B. E. Sernelius, *Phys. Rev. B* **24**, 1971 (1981).
- <sup>6</sup> W. P. Dumke, *Appl. Phys. Lett.* **42**, 196 (1983).
- <sup>7</sup> K. E. Newman, A. Lastras-Martinez, B. Kramer, S. A. Barnett, M. A. Ray, J. D. Dow, J. E. Greene, and P. M. Raccach, *Phys. Rev. Lett.* **50**, 1466 (1983).
- <sup>8</sup> Landolt-Börnstein, *Numerical Data and Functional Relationships in Science and Technology*, New Series, edited by O. Mandelung (Springer, Berlin, 1987).
- <sup>9</sup> B. E. Sernelius, K.-F. Berggren, Z.-C. Jin, I. Hamberg, and C. G. Granquist, *Phys. Rev. B* **37**, 10244 (1988).
- <sup>10</sup> J. Wagner and J. A. del Alamo, *J. Appl. Phys.* **63**, 425 (1988).
- <sup>11</sup> S. Permogorov and A. Reznitzky, *J. Lumin.* **52**, 201 (1992).
- <sup>12</sup> M. Weinstein, G. A. Wolf, and B. N. Das, *Appl. Phys. Lett.* **6**, 173 (1965).
- <sup>13</sup> M. Cardona, M. Weinstein, and G. A. Wolff, *Phys. Rev.* **140**, A633 (1965).
- <sup>14</sup> E. L. Lind and R. H. J. Bube, *J. Chem. Phys.* **37**, 2499 (1962).
- <sup>15</sup> C. A. Escoffery, *Appl. Phys. Lett.* **6**, 75 (1965).
- <sup>16</sup> M. Balkanski, A. Aziza, and E. Amzallag, *Phys. Status Solidi* **31**, 323 (1969).
- <sup>17</sup> M. Nagao and S. Watanabe, *Jpn. J. Appl. Phys.* **7**, 684 (1968).
- <sup>18</sup> R. L. Call, N. K. Jaber, K. Seshan, and J. R. Whyte, *J. Solar Energy Mater.* **2**, 373 (1980).
- <sup>19</sup> M. Jimenez-Garcia, G. Martinez, J. L. Martinez, E. Gomez, and A. Zehe, *J. Electrochem. Soc.* **131**, 2974 (1984).
- <sup>20</sup> 10-454 ASTM X-Ray Powder Data File.
- <sup>21</sup> 6-0314 ASTM X-Ray Powder Data File.
- <sup>22</sup> P. B. Allen and M. Cardona, *Phys. Rev. B* **23**, 1495 (1981); **24**, 7479 (1981).
- <sup>23</sup> I. Hamberg and C. G. Granquist, *J. Appl. Phys.* **60**, R123 (1986).
- <sup>24</sup> A. Ferreira da Silva, *Phys. Rev. B* **48**, 1921 (1993).